كلية الهندسة بشبرا
FACULTY OF ENGINEERING AT SHOUBRA
ERJ
PRINT ISSN 3009-6049
ONLINE ISSN 3009-6022

ENGINEERING RESEARCH JOURNAL (ERJ)
Volume (52),Issue (4)
October 2023, pp:38-47
https://erjsh.journals.ekb.eg

Flexural Behavior of Steel and FRP-Reinforced Geopolymer Concrete Beams : Numerical Modeling and Analytical Study

Nadia O. Nofal [1], Hossam H. Ahmed [2], Gehan A. Hamdy [2] , Ali S. Shanour [2] , Salma G. Saad [2,*]

[1] Housing and Building National Research Centre, Giza, Egypt
[2] Department of Civil Engineering , Faculty of Engineering at Shoubra, Benha University, Shoubra, Cairo, Egypt.
**Corresponding author*

E-mail address: nadia_nofal@yahoo.com, hossam@heliopolis_hctc.com, gehan.hamdy@feng.bu.edu.eg, ali.shnor@feng.bu.edu.eg, salmagamal022@gmail.com

Abstract: Geopolymer concrete has developed as an environmentally sustainable construction material the gained importance due to its cement-free production process. This paper presents numerical modeling through nonlinear finite element analysis (NLFEA) of reinforced geopolymer concrete beams as well as an analytical study. The numerical modeling and nonlinear analysis are performed using commercial software ANSYS, made for previously tested geopolymer concrete (GC) beams with main reinforcement bars of steel and glass fiber reinforced polymers (GFRP), and contains two types of dispersed fibers: steel and polypropylene fibers. The numerical results are presented and compared with the published experimental findings. A reasonable correlation between numerical and experimental results is observed, thus validating the efficiency of the modeling methodology for analyzing and designing geopolymer concrete c elements .

Keywords: Geopolymer concrete; beams; GFRP bars; numerical modeling; nonlinear analysis.

1. Introduction

Geopolymer concrete eliminates the use of cement and is thus regarded as an eco-friendly and sustainable construction material and is increasingly gaining acceptance [1-4]. Geopolymer concrete (GC) had been applied as reinforced concrete (RC) beams and the behavior was found by several researchers similar to conventional RC beams [5-7]. However, many reinforced concrete guidelines do not address the design of geopolymer concrete members, and therefore more investigation is needed to aid in developing adequate design formulas. It is always useful to be able to correctly simulate the structural behavior of such elements and analyze them numerically to avoid going through expensive experimental testing. The finite element method has been successfully applied for analysis of nearly all structural engineering problems and the method is implemented in many commercial computer software packages. Geopolymer concrete beams have been analyzed numerically by nonlinear finite element analysis (NLFEA) using in-house programs [7] or commercial software packages [8]; the resulting deflections were found to be similar to the experimental results [6-10]. Hassan et al. [11] investigated GC beams containing steel fibers experimentally and numerically using the nonlinear finite element analysis software ABAQUS 6.11 [12] and showed that compressive strength and stiffness increased due to the incorporation of steel fibers. [13] showed that GC beams displayed slightly higher deflection for the same amount of load compared to normal concrete beams. To increase beam flexural strength and ductility while providing corrosion protection, several researchers proposed using hybrid systems that combine steel and FRP bars as reinforcement [14-16]. The ductility of RC structures is increased using steel reinforcing bars, allowing tension failure, and preventing compression failure. [17] investigated geopolymer concrete beams and showed similar flexural, shear, and crack development to ordinary beams. [18] conducted experimental and computational analysis and demonstrated an increase in the moment capacity with an increase in steel reinforcement ratio. Concrete at the pressure zone of the surface caused the beams to fracture when their steel yielded first [19]. The numerical simulation provided higher stiffness than the theoretical calculation [20]. [21] investigated the flexural behavior of GC beams using the finite element method and reported experimental variations different from those that [22] had attempted to model using ANSYS 12.0 software, additionally, 20% discrepancy between experimental and numerical results was reported.

This paper presents numerical modeling using nonlinear finite element analysis (NLFEA) using ANSYS software version ANSYS 2021 R1 [23] for geopolymer concrete beams reinforced by steel bars and GFRP bars which have been previously tested experimentally [24]. The numerical modeling procedure, numerical results, and discussion as well as the analytical investigation are described in the following sections.

2. NUMERICAL MODELING AND FINITE ELEMENT ANALYSIS

Numerical modeling and nonlinear finite element analysis (NLFEA) were conducted using commercial software ANSYS, version ANSYS21 [23], to evaluate the flexural behavior of geopolymer-reinforced concrete (RC) beams that have been experimentally tested by the authors

[24]. The analyzed beams have dimensions 2000 mm, 150 mm, and 250 mm; the beam's dimensions and reinforcement details are shown in Figs. 1 and 2. The shear reinforcement of all beams is 8 mm diameter steel stirrups. Beams of group I are reinforced with steel bars, normal concrete beam B1 serves as control while B2, B3, and B4 are GC with increasing reinforcement ratios. Geopolymer concrete beams of Group II beams B5 to B8 have different reinforcement ratios of GFRP bars. Group III GC beams B9 and B10 reinforced by GFRP bars have steel and polypropylene fibers added to the GC mix.

The numerically evaluated behavior is compared with the experimental results in the following sections to validate the numerical modeling procedure.

2.1 Finite elements

Three finite element (FE) types were used for the idealization of the reinforced concrete beam, shown in Fig. 3. Concrete was modeled by element SOLID 65 having eight nodes each can experience x, y, and z directions displacements; the element has the capabilities of cracking, crushing, and deforming plastically. The reinforcing bars and stirrups are idealized by element LINK 180 3-D, capable of plastic deformation, and described by two nodes with x, y, and z translations at each node. The steel plates placed for loading and at supports are modeled by eight-node solid element SOLID 45. Three materials for rebars may be entered by the user representing directions x, y, and z in the smeared model.

2.2 Reinforcement-Concrete Interface

For representing the reinforcement in NLFEA, two approaches are commonly followed: discrete modeling (DM) and smeared modeling (SM). In SM, the reinforcement is uniformly distributed within the elements in a defined region of FE mesh, shown in Fig. 4(a) [25]; which is suitable for modeling the volumetric ratio for fiber reinforcement. In DM, reinforcement elements are connected to the concrete element at the same nodes of the concrete element, as shown in Figure 4(b); this model is adopted for the main longitudinal bars.

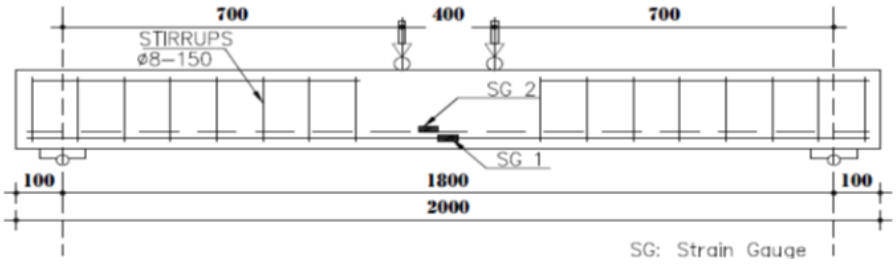

Fig 1. Geometry of the tested beams.

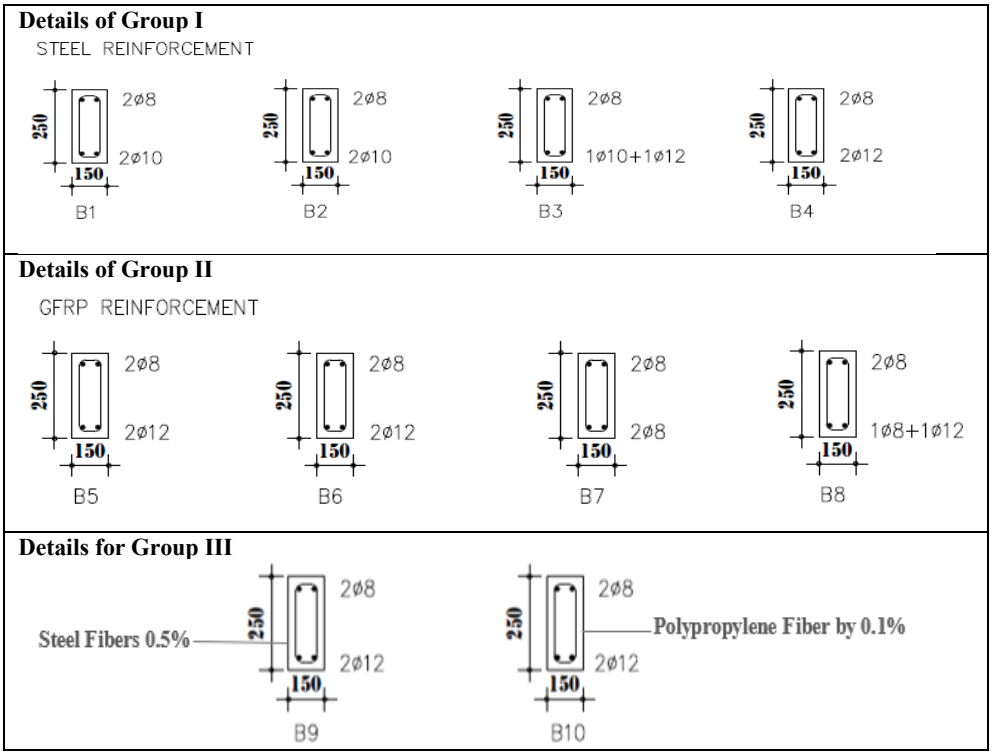

Fig 2. Details of reinforcement for the tested beams B1 to B10.

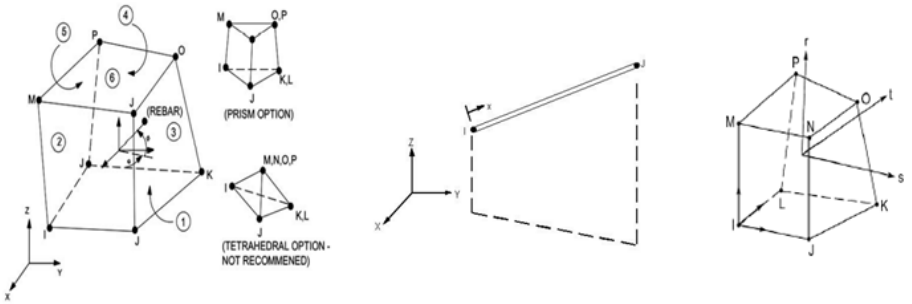

Fig 3. Adopted elements for modeling [23].

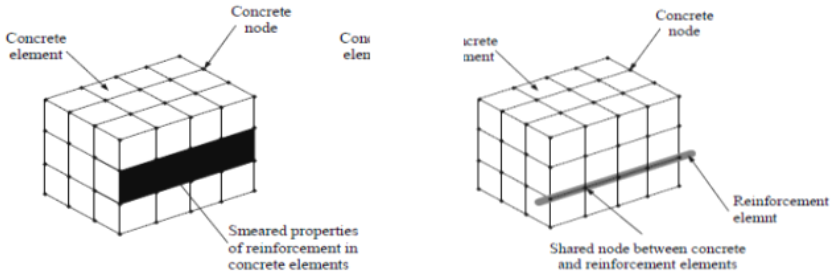

Fig 4. Modeling approaches for reinforcement [25].

2.3 Finite element models for beams

Ten three-dimensional FE models were made for GC beams with main reinforcement of steel or GFRP bars previously tested by the authors in bending until failure. The 3D FE models represent closely the beam's geometry, material properties, reinforcement details, boundary conditions, and loading, as shown in Fig 5.

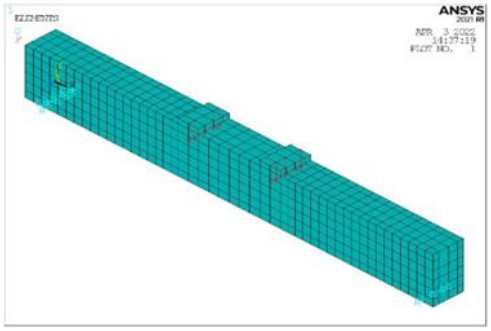

(a) Model of concrete beam and supports.

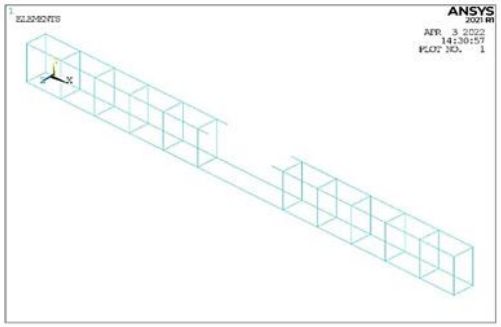

(b) Model of reinforcement.

Fig 5. Finite element model of a typical beam.

2.4 Adopted properties of materials

The material properties for normal concrete, GC, steel, and GFRP bars adopted in the FE simulation are given in Tables 1-3. Also, the adopted stress-strain curves are shown in Fig. 6.

TABLE 1. Material properties adopted for normal and geopolymer concrete.

Item	Normal concrete	Geopolymer concrete
Element Type	Solid65	Solid65
Modulus of elasticity (EX) (N/mm^2)	31116	32147
Passion ratio (PRXY)	0.2	0.2
Open crack shear coefficient	0.6	0.6
Closed crack shear coefficient	0.8	0.8
Uniaxial cracking stress (f_{ctr}) (N/mm^2)	5	5.388
Uniaxial crushing stress (f_{cu}) (N/mm^2)	50	53.88
Tensile crack factor	0.6	0.6

TABLE 2. Material properties for steel reinforcement.

Item	Main steel bars	stirrups
Modulus of elasticity (EX) (N/mm2)	200000	200000
Passion ratio (PRXY)	0.3	0.3
Yield stress (fy) (N/mm2)	420	280
Tan modulus (N/mm2)	10000	10000

TABLE 3. Properties of GFRP bars.

Diameter (mm)	Ultimate tensile strength fu (N/mm²)	Elastic modulus Ef (kN/mm²)	Rupture strain Ɛfu
8	680	44	0.02
12	700	45	0.02

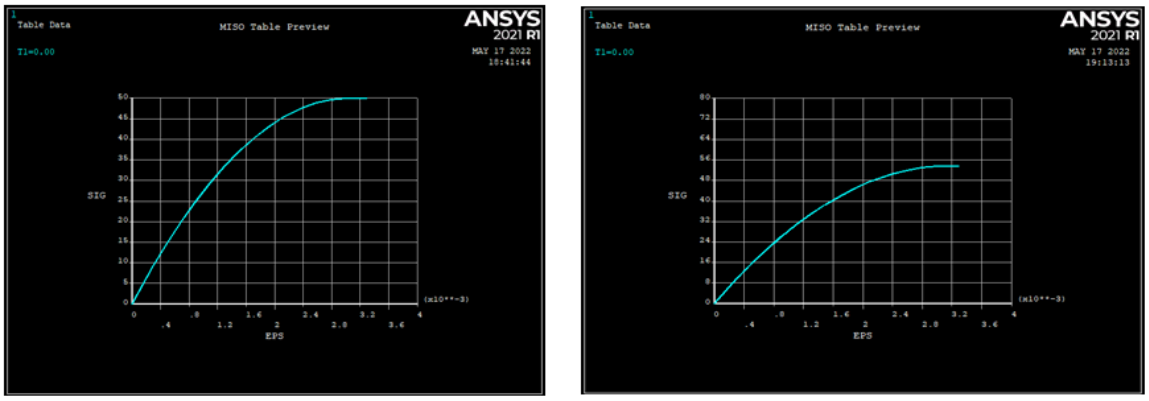

a. Normal concrete. b. Geopolymer concrete.

Fig 6. Stress-strain relations.

2.5 Steel reinforcement

The stress-strain relationship for longitudinal steel bars and stirrups is a bi-linear kinematic hardening relation, represented by two straight lines as shown in Fig. 7(a). The average stress-strain relation is expressed as follows.

For $\varepsilon_s \le \varepsilon_n$, $f_s = E_s \varepsilon_s$ (1)

And for $\varepsilon_s \ge \varepsilon_n$,

$$f_s = f_y \left[(0.91 - 2B) + \left(0.02 + 0.25B \frac{\varepsilon_s}{\varepsilon_y} \right) \right] \quad (2)$$

Where $\varepsilon_n = \varepsilon_y (0.93 - 2B)$ (3)

Parameter B is given as $\left(f_{cr} / f_y \right)^{1.5} / \rho$ (4)

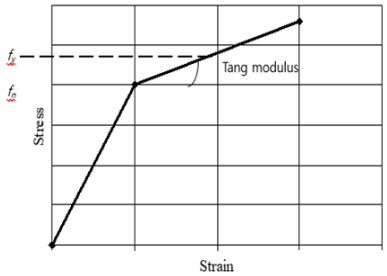

a. Steel reinforcement bars.

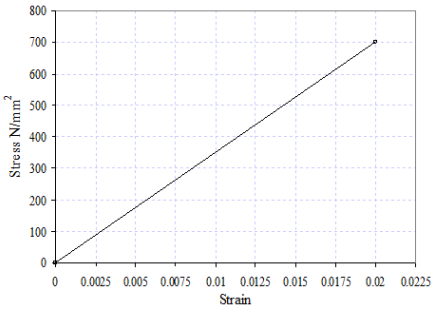

b. GFRP bars.

Fig 7. Stress-strain relations for steel and GFRP reinforcement.

2.6 GFRP Reinforcement

GFRP bars are modeled using FE used for steel reinforcement, LINK180, defined by linear-elastic properties determined experimentally and given in Table 3, and the stress-strain relation is shown in Fig. 7(b).

3. NUMERICAL Results And DISCUSSION

The numerical results obtained from NLFEA of the ten beams are given and are compared to the experimental results in Table 4. The relationship between load and mid-span deflection is plotted in Figs. 8 to 11 compared to those of the experimentally tested beams. Additionally, the experimental cracking patterns are depicted and compared

to the numerically predicted cracks at failure. The first cracks occur in the tension side of the beam in its middle third, i.e. the pure bending zone, when the concrete tensile strength or cracking strength is reached. By increasing the applied load, the beam cross-section neutral axis is shifted upwards towards the compressed side of the beam; cracks increase in width, length, and number until failure occurs by crushing of concrete on the compression side. Similar observations were reported by Hammad et al. [26]. The deformed shape of normal concrete beam B1 at failure is shown in Fig. 12; the maximum mid-span deflection is 15.19 mm.

TABLE 4. Numerical results of all studied beams.

Group	Beam	Concrete type	f_c (N/mm²)	Longitudinal reinforcement type	Fiber Ratio %	Numerical results		Experimental results		Numerical / experimental results	
						$P_{cr\ num}$ (kN)	$P_{u\ num}$ (kN)	$P_{cr\ exp}$ (kN)	$P_{f\ exp}$ (kN)	$P_{cr\ num}$ / $P_{cr\ exp}$	$P_{u\ num}$ / $P_{f\ exp}$
I	B1	N	50.5	Steel	0	26	54	15.57	56.72	1.67	0.95
	B2	G	53.8	Steel	0	28	62	18.21	61.7	1.54	1.00
	B3	G	53.8	Steel	0	28	72	22.5	82.83	1.24	0.87
	B4	G	53.8	Steel	0	28	78	23.03	85.94	1.22	0.91
II	B5	N	50.5	GFRP	0	24	66	19.78	95.59	1.21	0.69
	B6	G	53.8	GFRP	0	26	70	13.42	97.06	1.94	0.72
	B7	G	53.8	GFRP	0	26	35	11.21	45.09	2.32	0.78
	B8	G	53.8	GFRP	0	26	56	12.79	53.41	2.03	1.05
III	B9	G	53.8	GFRP + Steel Fibers	0.5%	26	108	16.31	104.92	1.59	1.03
	B10	G	53.8	GFRP + PP Fibers	0.1%	26	80	16.52	107.25	1.57	0.75

The variations in the results also show in Table 4 that when the reinforcement ratio decreases, cracking loads increase. And there is a small difference between the ultimate load for geopolymer concrete and normal concrete reinforcement by GFRP bars at the same ratio.

3.1 Cracking Loads

The observed cracking pattern and crack propagation were similar for all the tested beams: cracks appeared first at the tension bottom face of the beam in the constant moment region. The NLFEA also predicted crack formation in the studied beams when the applied load was in the range of 24 – 28 kN. From examining Table 4, good agreement is observed between the predicted and experimentally evaluated cracking loads with a mean ratio between them of 1.63 and a coefficient of variation (C.O.V) = 0.049 %.

3.2 Ultimate Capacity

The numerically evaluated ultimate loads show reasonable agreement with the experimental results, as observed from Table 4; the ratio of calculated to experimental results ranged between 0.72 and 1.05, with C.O.V of 0.93%, thereby validating the adopted modeling and NLFEA procedure.

3.3 Load – Displacement Behavior

Figures 8 to 10 show the relations for steel and GFRP reinforced beams between the applied load and the deflections measured at the mid-span of the beams. Generally, an acceptable agreement is observed between the plotted experimental and numerical values. In the linear range, the numerical load-deflection curves are coinciding with the experimental ones. After cracking, the stiffness of the FE models exceeds the experimental values due to the assumption of the perfect bond between concrete and reinforcement in FE analysis. This assumption is not valid for the experimental beams, since after cracking slight bond slip occurs resulting in loss of the composite action between the concrete and GFRP bars; leading to a decrease of the beam's overall stiffness than for the finite element models. El-Mogy [25] accounted for the bond-slip relationship by connecting the reinforcement and concrete elements nodes through non-linear spring elements. The FE model of this work succeeded to predict GC beam reinforced by GFRP bars up to 85% of the failure load.

3.4 Effect of addition of fibers to GC mix

For beams B9 and B10 with steel and polypropylene fibers added to the GC mix, the load mid-span deflection relations are plotted in Fig. 11 compared to GC beam B6 reinforced by GFRP bars. As observed from Fig. 11 and Table 4, the addition of steel fibers to the GC mix of GFRP-reinforced beams managed to increase the maximum load and deflection by 9% and 7%, respectively. Also, the addition of polypropylene fibers is observed to increase the maximum load and deflection by 10.6% and 4%, respectively, thus providing slightly more flexural capacity and ductility to the beam.

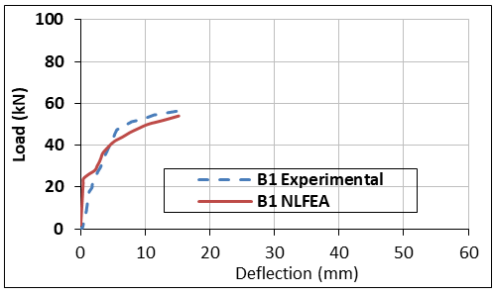

(a) Beam B1.

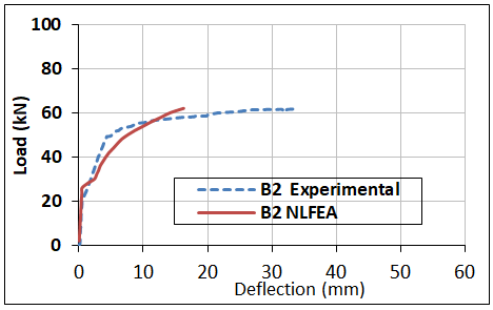

(b) Beam B2.

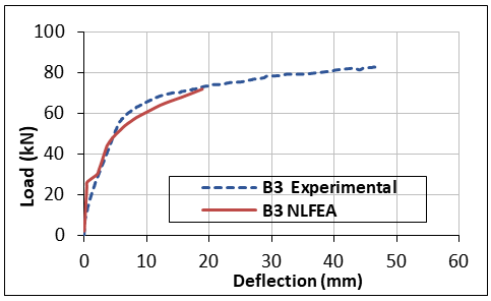

(c) Beam B3

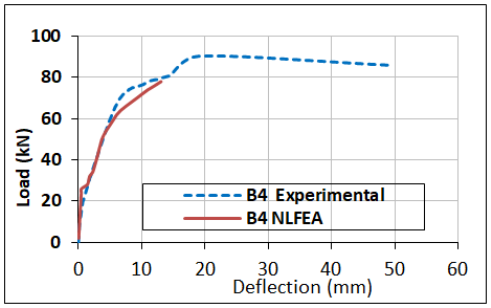

(d) Beam B4

Fig 8. Load-mid-span deflection relations for beams B1-B4.

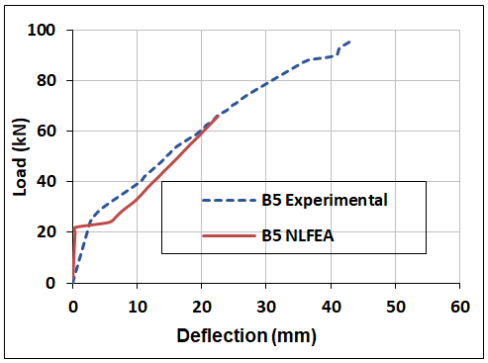

(a) Beam B5

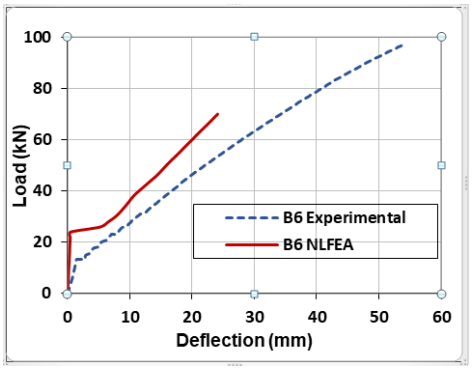

(b) Beam B6

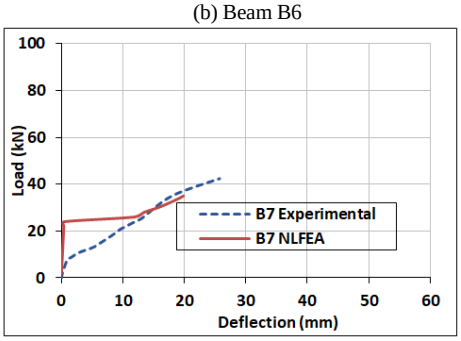

(c) Beam B7

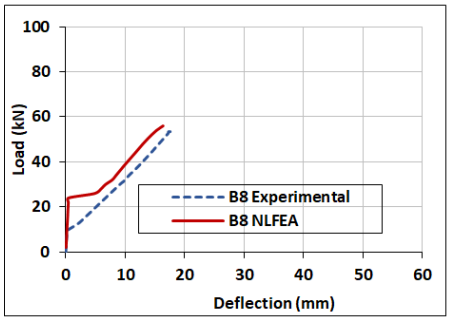

(d) Beam B8

Fig 9. Load-mid-span deflection relations for beams B5-B8.

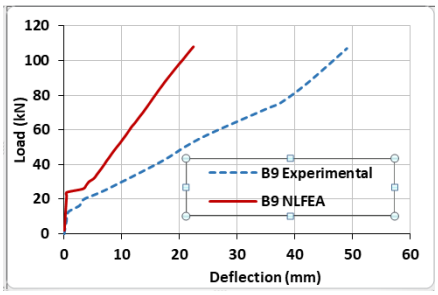

(a) Beam B9

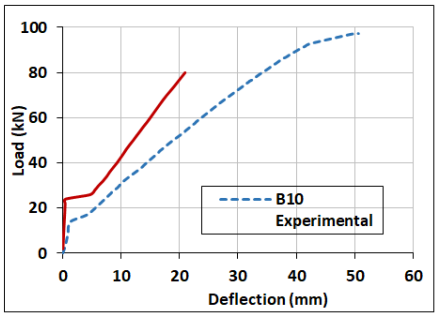

(b) Beam B10

Fig 10. Load-mid-span deflection relations for beams B9 and B10.

3.5 Cracking Patterns and Failure Modes

The experimentally observed cracking patterns and the cracks predicted numerically by NLFEA for beam B1 are shown in Fig. 12, at the first crack, at 50% of the ultimate load, and failure. The cracking patterns and the failure modes for GC beams were nearly the same as those of ordinary concrete beams. Also, agreement was achieved between the cracks obtained by numerical analysis and the experimentally observed crack patterns.

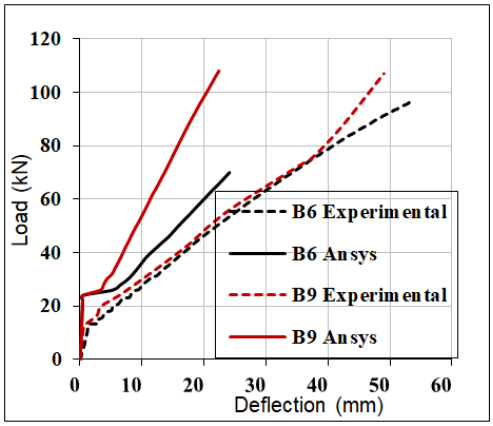

(a) Addition of steel fibers.

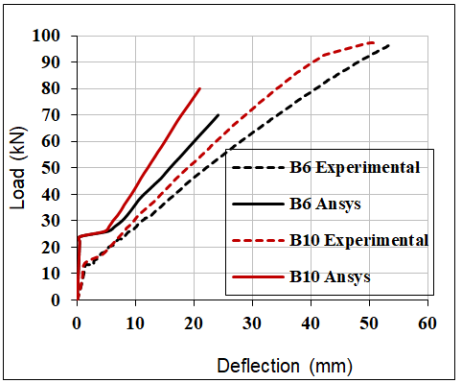

(b) Addition of pp fibers.

Fig 11. Influence of addition of fibers to geopolymer concrete beams.

4. ANALYTICAL CALCULATION OF FLEXURAL CAPACITY

Using the equivalent rectangular stress block as the base for calculating the flexure capacity of the beam cross-section, sketched in Fig. 13, the compression zone height, equivalent rectangular stress block, and ultimate capacity can be calculated by the force and moment equilibrium condition.

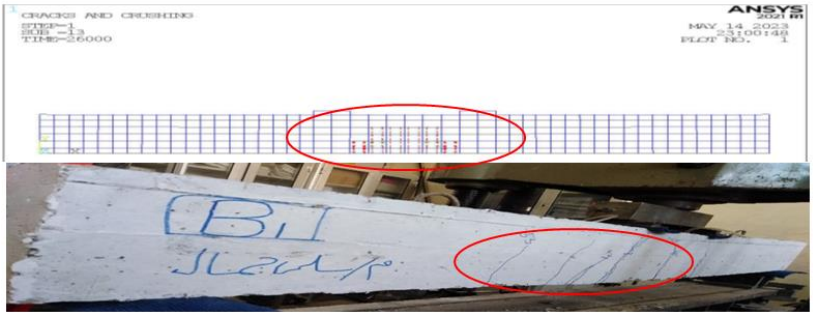

(a) at cracking load P_{cr}

(b) at 50% of Pf

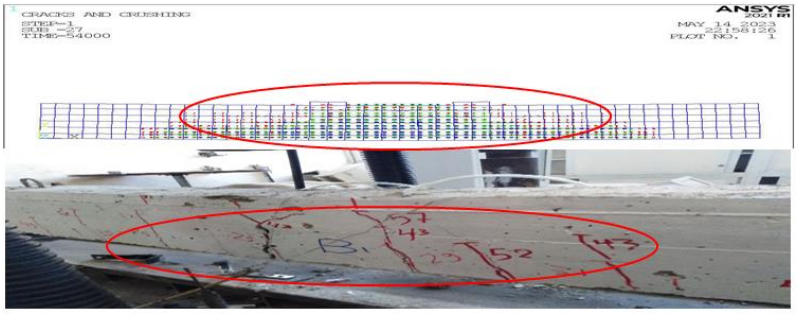

(c) at failure

Fig 12. Cracks propagation for beam B1.

$$\sum X = 0 \qquad \alpha_1 f_c b x = f_y A_s \qquad (4)$$

$$\sum M = 0 \qquad M_u = \alpha_1 f_c b x (h_0 - \frac{x}{2}) \qquad (5)$$

Where: M_u is the flexural capacity of the normal section of the tested beam, f_c is the concrete compressive strength (MPa), f_y is the tensile strength for steel (MPa), $\alpha_1$is the equivalent rectangular stress diagram coefficient of concrete in the compression zone. According to the technical standard of geopolymer concrete, the assumed value of $\alpha_1$for this kind of concrete is 0.90.

Also, h_o is the effective height, h_o = h - a_s , where a_s = c + d_v + $d/2$

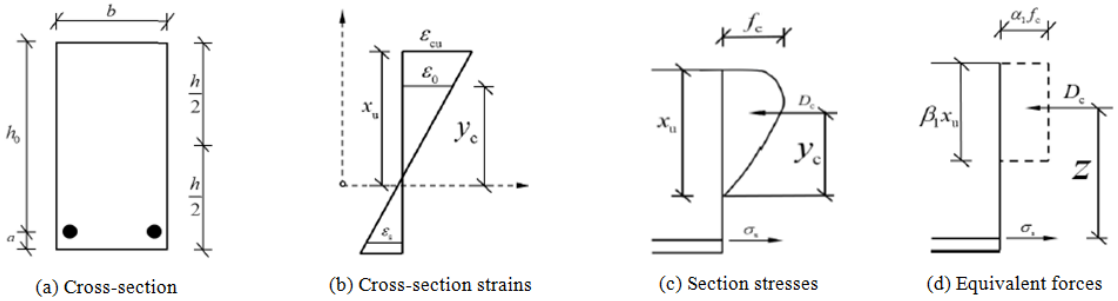

Fig 13. Analysis of beam cross-section at failure.

Table 5. The analytical and experimental ultimate capacity of all beams.

Beam	M_u	$M_{u\,exp}$	$M_{u\,exp}/M_u$
B1	54.5	56.72	1.04
B2	54.8	61.70	1.12
B3	66.5	82.83	1.25
B4	78.8	85.94	1.09
PCC-18-1.20 [Ref.27]	60.3	66.20	1.10
PCC-25-1.20 [Ref. 27]	65.5	69.9	1.07
PCC-33-1.20 [Ref. 27]	69.4	73.6	1.06
PC-RHA-18-1.2 [Ref. 27]	60.1	64.9	1.08
PC-RHA-25-1.2 [Ref. 27]	65.4	69.5	1.06
PC-RHA-32-1.2 [Ref. 27]	69.1	72.5	1.05

Average value x=1.092, stand. dev. σ=0.98, COV =0.01.

The parameters of each tested beam are substituted into the above equation to calculate the ultimate moment capacity Mu. The calculated and experimental results are listed in Table 5, together with results obtained by Thumrongvut et al. [27]. It is observed that the predicted values of the beam's ultimate flexural capacity Mu are close to the experimental values, therefore the presented formula can be effectively applied to determine the ultimate capacity of GC flexural elements. The flexural capacity increases with increasing the reinforcement ratio: the calculated ultimate moment of beam B4 is 22.31% higher than that of beam B2 due to the increasing reinforcement ratio from ρ =0.48% to ρ =0.58%. Furthermore, as observed from Table 5, the numerical results approach the experimental values for higher reinforcement ratios.

Conclusions

In this paper, numerical modeling was made for geopolymer concrete (GC) beams with different reinforcement schemes. Numerical modeling and nonlinear finite element analysis (NLFEA) were performed using commercial software ANSYS for GC beams having main tensile reinforcement of steel or GFRP bars and with the addition of steel or polypropylene fibers to the concrete mix that has been experimentally tested by the authors under four-point loading until failure. The numerical models were compared to the experimental results. Additionally, the flexural capacity of the beams was estimated by analysis of the ultimate moment of the beam cross-section. The main conclusions reached by this study can be summarized in the following points.

- Numerical modeling and nonlinear analysis were performed to study the flexural behavior of GC beams using a commercially available nonlinear analysis software ANSYS, which enables any practicing engineer to perform the analysis.
- The numerical results obtained in this study by NLFEA are in good agreement with the experimental results regarding first crack loads, moment-carrying capacity, and load-deflection

response.

- The numerically predicted flexural capacity of GC beams increases as their reinforcement ratio increases.
- The failure occurred in flexure mode for all the GC beams, where cracks initiated from the center of the tension face of the beams; by increasing the load, cracks increased in number and width and propagated until reaching the compression zone of the beams.
- It has been noticed that the formation of flexural cracks is substantially fewer in GC beams compared to conventional reinforced concrete beams.
- The addition of steel and polypropylene fibers to GC beams reinforced by GFRP contributed very slightly to the improvement of the flexural behavior. The increase in the ultimate load was 9% and 10.6%, and the increase in maximum deflection was 7% and 4% for steel and polypropylene fibers addition, respectively, providing the beam with slightly more flexural capacity and ductility.
- The analysis made for GC beams cross sections to evaluate the ultimate moment yielded values that are close to the experimental values; indicating that the presented formulas can reliably determine the flexural capacity of geopolymer concrete flexural members.
- There is currently limited information available on the mechanical behavior of the presence of steel fibers within the geopolymer concrete mix and its impact on the related structural performance of geopolymer reinforced concrete beams of T-section. But more study is required to take cyclic load behavior and torsional behavior of GC reinforced beams into account.
- Therefore, it is highly advised that cement be replaced in new construction with geopolymer concrete made from locally available materials in Egypt.

Notations:

GC	geopolymer concrete
GFRP	glass fiber reinforced polymers
NLFEA	nonlinear finite element analysis
P_{cr}	cracking load of the beam
P_u	ultimate numerical load of the beam
P_f	failure load of the beam
δ_u	deflection of the beam at the maximum numerical load
δ_f	deflection of the beam at the failure load
f_c	concrete compressive strength (MPa)
f_{cr}	cracking strength of concrete (MPa)
f_y	tensile strength for steel (MPa)
f_s	average stress in steel bar (MPa)
ε_y	average strain in steel bar
E_s	Young's modulus of steel reinforcement
h_o	effective height of beam cross-section
α_1	equivalent rectangular stress diagram coefficient
M_u	flexural capacity of the middle section of the tested beam
ρ	reinforcement ratio
f_y	yield stress of steel bar
ε_y	yield strain of steel bar

REFERENCES

[1] S. Parathi, P. Nagarajan and S.A. Pallikkara, Ecofriendly geopolymer concrete: A comprehensive review. Clean Techn Environ Policy 23, 1701–1713 (2021). https://doi.org/10.1007/s10098-021-02085-0

[2] T. Lingyu, H. Dongpo, Z. Jianing and W. Hongguang, Durability of geopolymers and geopolymer concretes: A review, Rev. Adv. Mater. Sci. 2021; 60:1–14. https://doi.org/10.1515/rams-2021-0002

[3] A. Esparham and F. Ghalatian, The features of geopolymer concrete as a novel approach for utilization in green urban structures, Journal of Composites and Compounds 4 (2022) 89-96.

[4] N. Li, C. Shi, Z. Zhang, H. Wang and Y. Liu, A review on mixture design methods for geopolymer concrete, Compos. Part B: Eng 178, 2019, 107490.
https://doi.org/10.1016/j.compositesb.2019.107490

[5] A. Hutagi and R. B. Khadiranaikar, Flexural behavior of reinforced geopolymer concrete beams, Inter. Conf. Electrical, Electronics, and Optimization Techniques (ICEEOT), Chennai, India, 2016, 3463-3467.

[6] M. A. Saeed, A.S.A. Al Amli, Structural behavior of geopolymer reinforced concrete beams: A short review, J. Eng. Sus. Develop. 27(1), 80–94, 2023.

[7] Y.N. Wibowo, B. Piscesa, Y. Tajunnisa, Numerical investigation of geopolymer reinforced concrete beams under flexural loading using finite element analysis, J Civ. Eng., 37 (1), June 2022.

[8] B. Sarath Chandra Kumar and K. Ramesh, Analytical study on flexural behaviour of reinforced geopolymer concrete beams by ANSYS, IOP Conf. Ser.: Mater. Sci. Eng., 455(1), 2018, 012065.

[9] O. Hameed, Z. Alridha, M. Alhawat, Numerical and theoretical analysis of FRP reinforced geopolymer concrete beams, Case Stud. Constr. Mater.,16, March 2022.

[10] Q. Pham, T. N. Nguyen, S. T. Le, T. T. Pham, and T. D. Ngo, Experimental and analytical investigations on shear behaviour of reinforced geopolymer concrete beams, Int. J. Civ. Struct. Eng., 2, ISSN 0976 – 439, 2011.

[11] A. Hassan, M. Arif, M. Shariq, Experimental test and finite element modelling prediction on geopolymer concrete beams subject to flexural loading. Innov. Infrastruct. Solut. 7(13), 2022. https://doi.org/10.1007/s41062-021-00615-9

[12] ABAQUS 6.11 theory manual Simulia (2017) Abaqus 6.11 theory manual. DS SIMULIA Corp, Providence, RI, USA.

[13] P. Ambily, C. K. Madheswaran, N. Lakhsmanan, J. K. Dattatreya, S. A. J. Sathik, Experimental studies on shear behaviour of reinforced geopolymer concrete thin webbed T-beams with and without fibres, Inter. J. Civ. Struc. Eng., 2012.

[14] I. F. Kara, A. F. Ashour, M. A. Körog˘lu, Flexural behavior of hybrid FRP/steel reinforced concrete beams, Compos. Struct., 129, 111–121, 2015.

[15] Z. Sun, L. Fu, D.-C. Feng, A. R. Vatuloka, Y. Wei, G. Wu, Experimental study on the flexural behavior of concrete beams reinforced with bundled hybrid steel/ FRP bars, Eng. Struct., 197, 2019.

[16] W.-J. Ge, A. F. Ashour, J. Yu, P. Gao, D.-F. Cao, X. J. C. Cai, Flexural behavior of ECC–concrete hybrid composite beams reinforced with FRP and steel bars, J. Compos. Constr., 23 (1), p. 04018069, 2019.

[17] A.İ. Çelik , A. Özbayrak, A. Şener , M.C. Acar, Numerical analysis of flexural and shear behaviors of geopolymer concrete

beams, J Sustain Const Mater Technol, 7(2), 70–80, 2022. http://doi.org/10.14744/jscmt.2022.13

[18] T. T. Pham, D. Q., Nguyen, T. N., Le, S. T., Pham T. D. Ngo, The structural behaviours of steel reinforced geopolymer concrete beams: An experimental and numerical investigation, Struct., 33, 567–580, 2021.

[19] P. U. Kumar and B. S. C. Kumar, Flexural behavior of reinforced geopolymer concrete beams with GGBS and metakaoline, Inter. J. Civ. Eng. Tech., 7(6), 260–277, 2016.

[20] K.T. Nguyen, N. Ahn, T.A. Le, K. Lee, Theoretical and experimental study on mechanical properties and flexural strength of fly ash-geopolymer concrete, Construc. Build. Mater., 106, 65–77, 2016.

[21] A. M. Amiri, A. Olfati, S. Najjar, P. Beiranvand, M. N. Fard, The effect of fly ash on flexural capacity concrete beams, Adv. Sci. Tech. Res. Jo., 10(3), 89–95, 2016.

[22] K. Uma, R. Anuradha, R. Venkatasubramani, Experimental investigation and analytical modeling of reinforced geopolymer concrete beam, Int. J. Civ. Struct. Eng., 2(3), 2012.

[23] ANSYS21 Manual Set, ANSYS Inc., South Pointe Technology Drive,

FLEXLIM License Manager Canosburg, PA, U.S.A, 2021.

[24] N.O. Nofal, H.H. Ahmed, G.A. Hamdy, A.S. Shanour and S.G. Saad, Experimental investigation of the flexural behavior of geopolymer concrete beams with different reinforcement schemes, Eng. Res. J. (ERJ), Faculty of Engineering at Shoubra, Benha University, 2023, under publication.

[25] M. A. T. El-Mogy, Behaviour of Continuous Concrete Beams Reinforced with

FRP Bars, Ph.D. Thesis, University of Manitoba ,Winnipeg, Manitoba, Canada, 2011.

[26] N. Hammad, A. El-Nemr, H. E. Hasan,The performance of fiber GGBS based alkali-activated concrete, J. Build. Eng. 42 (2021):102464. http://dx.doi.org/10.1016/j.jobe.2021.102464

[27] J. Thumrongvut, S. Seangatith, C. Phetchuay, C. Suksiripattanapong, Comparative Experimental Study of Sustainable Reinforced Portland Cement Concrete and Geopolymer Concrete Beams Using Rice Husk Ash. Sustainability 2022, 14, 9856.

https://doi.org/10.3390/su14169856